Electrochemiluminescence

DOI: 10.1002/ange.200802034

Tuning of Electrogenerated Silole Chemiluminescence**

Christina Booker, Xin Wang, Samar Haroun, Jigang Zhou, Michael Jennings, Brian L. Pagenkopf, and Zhifeng Ding**

Increasing interest in π-conjugated compounds containing silole rings (1-silacyclopentadiene)[1] is to a large extent due to recent exploitation for applications such as electrochemiluminescent sensors and light-emitting diodes.[2–10] Their unique photophysical and electronic properties[11] arise from the particularly low lying LUMO owing to σ*–π* conjugation between the σ* orbital of two exocyclic σ bonds on the silicon atom and the π* orbital of the butadiene moiety.[12,13] We recently reported the synthesis of donor–acceptor siloles[14] and oligomeric ethynyl siloles,[15] and the electrogenerated chemiluminescence (ECL)[16] of several silole-based chromophores.[17] We also reported a series of 2,5-bis(arylethynyl) siloles in which a curious improvement of photoluminescence (PL) quantum efficiency from 9 to 63% was achieved by increasing the steric bulk on the silicon atom and 2,5-substituents.[18] It seemed plausible that the enhanced luminescence resulting from the highly improved quantum efficiency was due to increasing the energy barriers for nonemissive decay processes. However, these electronic improvements did not translate to ECL, and the efficiencies of some ethylene- and ethynyl-substituted siloles[17] were only in the range of 0.001 to 0.1 relative to 9,10-diphenylanthracene (DPA),[19] owing to the instability of their radical cations needed for ECL generation.[20] Herein we report that successful tuning of the electrochemical potentials and of silole–thiophene hybrid chromophores results in higher stability of the radical cations and ultimately in improved ECL efficiency.

Considering that 1,1-dimethyl-2,5-bis(2-thienyl)-3,4-diphenylsilole (**3a**) and 1,1-dimethyl-2,5-bis[(2,2′-bithiophen)-5-yl]-3,4-diphenylsilole (**4a**) are efficient electron-transporting materials,[21] we expected that replacement of the methyl substituents with larger isopropyl, *tert*-butyl and *n*-hexyl groups would augment the energy barriers for nonemissive decay processes, stabilize the radical cations generated electrochemically, and thus result in enhanced photoluminescence and ECL. Therefore the target chromophores, **3b–d** and **4b–d**, were prepared as shown in Scheme 1. Intramolecular cyclization of bis(phenylethynyl) dialkyl

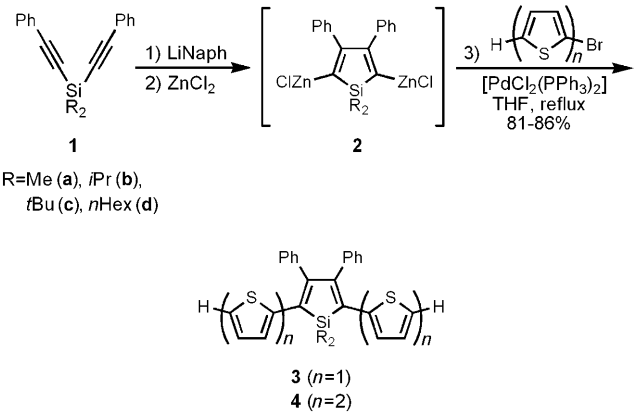

Scheme 1. Synthesis of thienyl-containing silole chromophores.

silanes **1** with an excess of lithium naphthalenide followed by reaction with $ZnCl_2$ afforded 2,5-dizinc intermediates **2**, which were used in situ to prepare silole chromophores **3** and **4** by Negishi cross-coupling reactions catalyzed by $[PdCl_2(PPh_3)_2]$.[15,22] Good yields were obtained by carrying out the entire reaction sequence, consisting of cycloreduction, transmetalation, and cross-coupling, from silane **1** to silole **3** or **4** in one pot.

Figure 1 shows cyclic voltammograms (CVs) of 0.78 mM **4a** (a) and 1.34 mM **4c** (b) in dichloromethane solution containing 0.1M tetrabutylammonium perchlorate as supporting electrolyte. Electrochemical data for the other six siloles are summarized in Table 1. As the potential is scanned from zero to the positive region, **4a** loses an electron to become a radical cation at a half-wave potential of 0.818 V, and loses a second electron to likely become a radical dication at a half-wave potential of 0.972 V (Figure 1a). The half-wave potentials for the two consecutive oxidations of **4c** are 0.697 and 0.840 V, respectively (Figure 1b). The calculated (DFT/B3LYP/6-31G*) electron density in the HOMOs of **4c** and its radical cation are spread out over the conjugated thiophene units. In the X-ray crystal structure of **4c** (Figure 2), the two bithiophenyl groups are almost in the same plane as the silole core. Coplanarity of silole and bithiophenyl moieties may lead to a second oxidation wave instead of one two-electron oxidation reaction, which agrees well with the results of quantum chemical calculation (see the Supporting Information). Because the conjugated system is so extensive in **4c**, the molecule can compensate for the missing

[*] C. Booker, X. Wang, S. Haroun, Dr. J. Zhou, Dr. M. Jennings, Prof. Dr. B. L. Pagenkopf, Prof. Dr. Z. Ding
Department of Chemistry, The University of Western Ontario
1151 Richmond St., London ON N6A5B7 (Canada)
Fax: (+1) 519-661-3022
E-mail: zfding@uwo.ca
bpagenko@uwo.ca
Homepage: http://www.uwo.ca/chem/

[**] This work was supported by NSERC, PREA, CFI, OIT, and UWO. We thank FMC Lithium, a division of FMC Corporation, for a generous donation of $tBu_2Si(OTf)_2$, and we thank Lindsay Kelland for ECL experiments.

Supporting information for this article is available on the WWW under http://dx.doi.org/10.1002/anie.200802034.

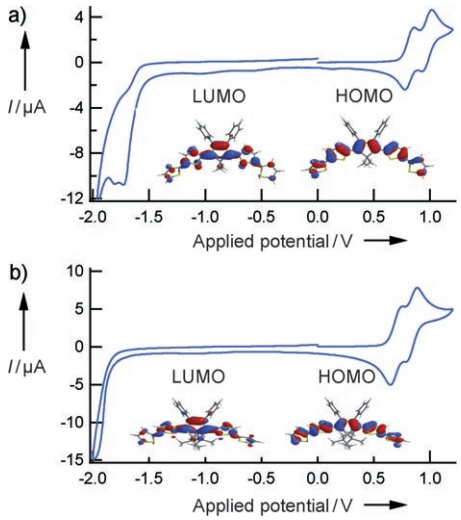

Figure 1. Cyclic voltammograms of 0.78 mM of **4a** (a) and 1.34 mM of **4c** (b) in CH_2Cl_2 with 0.1 M tetrabutylammonium perchlorate as supporting electrolyte. A Pt disk embedded in a glass tube was used as working electrode (0.03 cm^2), a Pt wire as counterelectrode, and a Ag wire as quasi-reference electrode. The scan rate was at 0.1 Vs^{-1}. Insets are molecular orbital isosurface plots for HOMOs and LUMOs based on the DFT/B3LYP/6-31G* calculations.

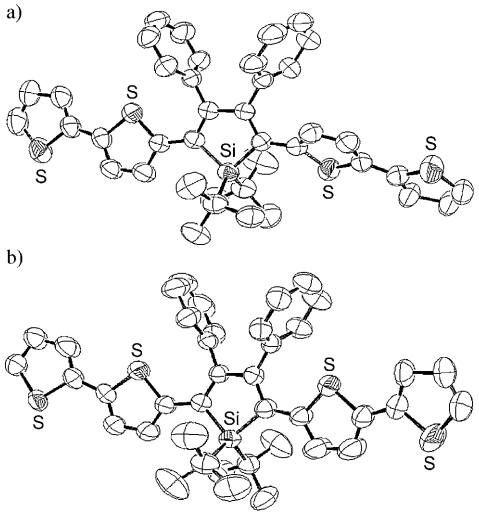

Figure 2. X-ray single-crystal structure of **4c** showing each of the crystallographically independent molecules with 50% probability displacement ellipsoids. H atoms have been omitted for clarity. CCDC-650096 contains the supplementary crystallographic data for this paper. These data can be obtained free of charge from The Cambridge Crystallographic Data Centre via www.ccdc.cam.ac.uk/data_request/cif.

Table 1: Energy levels of HOMOs and LUMOs, and redox peak potentials.[a]

	1st ox anod./ cathod. peaks [V]	2nd ox anod./ cathod. peaks [V]	1st red peak [V]	2nd red peak [V]	HOMO/ LUMO [eV][b]
3a	1.053/0.966	1.266/1.163	−1.850	−1.926	−4.95/ −1.82
3b	1.086/0.945	1.387/1.199	−1.907	−1.978	–
3c	1.166/1.069	1.416/1.260	–	–	−5.23/ −1.75
3d	1.087/0.932	1.417/1.228	−1.887	−1.958	–
4a	0.857/0.779	1.012/0.932	−1.724	−1.808	−4.72/ −2.06
4b	0.869/0.786	1.096/0.962	−1.741	−1.870	–
4c	0.744/0.649	0.887/0.793	−1.725	−1.806	−4.97/ −1.96
4d	0.853/0.782	1.091/0.949	−1.724	−1.778	–

[a] Other electrochemical conditions are the same as in Figure 1. [b] Energies obtained from the DFT/B3LYP/6-31G* calculations.

electron by sharing the remaining electron density over a more expansive molecular orbital. Therefore, the oxidation processes appear quasi-reversible in the cyclic voltammogram (Figure 1b). Compounds **4b** and **4d** show two reversible or quasi-reversible oxidation reactions (see the Supporting Information).

It is a little easier to oxidize **4c** than **4a, 4b**, and **4d** (Table 1) because *tert*-butyl is a better electron donor than the other alkyl groups. The two oxidation reactions of **4c** are less separated than those of the other three compounds. The bulky *tert*-butyl group seems to prevent resonance of the radical cation and make the two bithiophenyl behave independently on accepting an electron. Siloles **3a–3d** are more difficult to oxidize than their counterparts **4a–4d** because of less π conjugation, and the irreversibility of their oxidation reactions indicates instability of the cations formed (see the Supporting Information). New peaks that appeared when the applied potential was reversed from positive to 0 V indicate chemical reactions after electrochemical ones (EC mechanism). Regardless of these differences, the radical cations of all eight silole compounds are much more stable than those of ethylene- and ethynyl-substituted siloles,[17] and improved ECL efficiency of these compounds is anticipated.

On scanning the potential to negative, two consecutive cathodic peaks were observed for **4a** (Figure 1a), which suggest that two electrons were added sequentially to the silole ring during the reduction process to produce radical anions and dianions. This is similar to the alkali metal reduction of phenyl-substituted siloles.[23] In the calculated molecular orbital isosurface plots (inset in Figure 1a), localization of the LUMO around the central silole ring suggests electron addition to the silole ring, which agrees well with our electrochemical results. Interestingly, reduction of **4b**, **4c**, and **4d** (Table 1) is very similar to that of **4a** (first reduction peaks at −1.724, −1.741, −1.725, and −1.724 V for **4a–d**). The larger alkyl groups and sterically bulky *tert*-butyl group appear to have little effect on resistance to electron gain. The LUMO energies from the quantum calculations are very similar (−2.06 and −1.96 eV for **4a** and **4c**, respectively) and agree very well with the first-reduction peak potentials. Further reduction of the silole radical anion again likely proceeds on the silole moiety according to quantum chemical calculations (see the Supporting Information), which agrees well with the experimental results of chemical reduction of some siloles.[23] The peak potentials for the second reduction are also very similar, although the two successive reduction peaks are sometimes convoluted. Compounds **3a–d** are more difficult to reduce than their silole counterparts **4a–d** within the potential

window because of less conjugation in the system (see Table 1 and the Supporting Information). Well-defined reduction waves for **3c** can not be observed prior to reduction of the electrolyte solution. The reduction peak potentials for the other three siloles (**3a, 3b**, and **3d**) are very similar. The energies of frontier molecular orbitals for **3a** and **3c** are also listed in Table 1.

Figure 3 shows a CV overlaid with the simultaneous ECL photocurrent/voltage curve recorded for **4c**. This graph

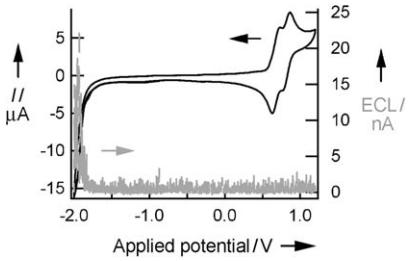

Figure 3. Cyclic voltammogram (black) and ECL–voltage curve (gray) of 1.34 mM **4c** in the second cycle scanned at 0.1 Vs^{-1}. Potential scan direction is the same as in Figure 1.

illustrates the typical light emission from a silole compound during potential scanning. The proposed mechanism for the ECL observed in the experiments is given in Equations (1)–(4).

$$\text{silole} + e^- \rightarrow \text{silole}^{\bullet -} \quad (1)$$

$$\text{silole} - e^- \rightarrow \text{silole}^{\bullet +} \quad (2)$$

$$\text{silole}^{\bullet -} + \text{silole}^{\bullet +} \rightarrow \text{silole}^* + \text{silole} \quad (3)$$

$$\text{silole}^* \rightarrow \text{silole} + h\nu \quad (4)$$

The radical anion that is formed in the region of negative potential reacts with the radical cation that is generated under positive potential. This annihilation reaction generates an excited silole species and a ground-state silole,[20] and the excited silole returns to ground state with emission of light. The ECL is formed when the potential sweeps through a full cycle, and the light is detected when the potential is scanned in the negative potential region. This provides an insight into the stability of the radical anions and cations, that is, the radical cations are more stable than the anions. This agrees well with the corresponding electrochemical behavior demonstrated in the CVs, where oxidation is quasi-reversible and reduction irreversible. For **4a, 4b**, and **4d**, ECL was detected in the region of negative potential as well. Compounds **3a–d** emit ECL in a similar way at a higher absolute potential than **4a–d**. This observation is paralleled by the shift in the corresponding oxidation peak potentials. Less energy is required to oxidize and reduce **4a–d** due to their more extended conjugated systems compared to **3a–d**. These thiophene-extended siloles show more stable ECL emission than ethylene- and ethynyl-substituted siloles.[17] This is expected from the quasi-reversible oxidation behavior resulting from the improved stability of the cation radicals. The ECL was enhanced when the working electrode was quickly pulsed between the first oxidation and reduction peak potentials with a pulse width of 0.1 s (Figure 4a) rather than the slow scanning in Figure 3. This allows greater numbers of radical cations and anions to meet in this process. The high temporal pace circumvents the decay of the relatively unstable radical anions before annihilation.

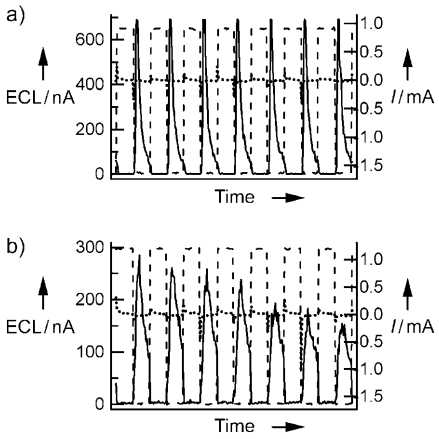

Figure 4. Curves of ECL intensity versus time (solid) and electrochemical current versus time (dotted) of **4a** along with the applied potential profiles (dashed), recorded during the process of pulsing the working electrode a) between the first reduction and oxidation potentials (−1.630 and 0.916 V) and b) between the first reduction and the second oxidation peak (−1.630 and 1.195 V) at a pulse width of 0.1 s.

The ECL efficiency was determined as the photons emitted per redox event relative to DPA (Table 2). Siloles **4a–d** clearly show higher ECL efficiency than **3a–d** due to their extended π conjugation. The ECL from **4a**, **4c**, and **4d** is almost twice as efficient as that from ethylene- and ethynyl-substituted siloles.[17]

Table 2: Spectroscopic data of the siloles.

	Absorption		Photoluminescence		Electrochemiluminescence		λ_{max}(ECL)−λ_{max}(PL)
	λ_{max} [nm]	$\varepsilon\times10^3$ [$M^{-1}cm^{-1}$]	λ_{max} [nm]	QE [%][a]	λ_{max} [nm]	QE [%][b]	[nm]
3a	414	9.72	514	0.34	595	0.40	81
3b	410	79.0	519	0.40	668	0.135	149
3c	381	6.26	524	1.73[c]	565	0.48	41
3d	416	207	519	0.48	590/712	2.3	77/203
4a	474	19.2	573	1.27	603	17.6	30
4b	471	91.0	580	1.82	693	12.5	113
4c	435	9.27	581	3.81	594	19.6	13
4d	476	213	574	2.11	596/722	24.9	22/148

[a] Quantum efficiency (QE) determined with respect to fluorescein unless otherwise indicated. [b] QE relative to the emission of DPA[19] under similar conditions. [c] Relative to DPA.

The recorded ECL intensities for all eight compounds excited by pulsing or scanning between the second oxidation and the second reduction peak potentials (Figure 4b) were lower than those obtained when the working electrode was pulsed or scanned between the first oxidation and reduction peak potentials (Figure 4a).

Moreover, in the wider range of pulsing potential, ECL was unstable and quickly decreased over time (Figure 4b), whereas the ECL efficiency remained constant when pulsing was limited to the first oxidation peak (Figure 4a). During the course of these experiments film formation at the electrode was observed in the wider sweep window, but not in the narrower. This observation suggests that the sustainable ECL observed here may be due to circumventing polymer formation from a dicationic intermediate, that is, participation of the radical cations generated after the first oxidation in the annihilation reaction with the radical anions results in efficient ECL, whereas the radical dications appear to engage in a separate reaction manifold resulting in electrode fouling and decreased ECL efficiency. The ECL efficiency was improved by tuning the potential range.

The ECL was also observed when the potential was cycled only through the negative potential region (0 to −2.5 V). This is not surprising, since Bard and co-workers[24] proposed that the dichloromethane solvent can decompose during these electrochemical experiments and act as a coreactant to generate ECL with the silole radical anions.

Figure 5 shows the ECL spectra of the eight siloles during pulsing of the working electrode in the redox potential ranges. The ECL peak wavelengths for **4a** and **4c** are slightly redshifted relative to the corresponding PL values, whereas the wavelength at ECL maximum is redshifted relative to that at the PL maximum for **4b** by as much as 113 nm (Table 2). The wavelength differences between ECL and PL maxima for **3a–c** are larger than those for **4a–c**, and this suggests that the former may undergo more nonradiant relaxation than the latter in the ECL processes. Peak wavelengths in ECL spectra for **3c** (565 nm) and **4c** (594 nm) are very close to those in the PL spectra (524 and 581 nm, respectively), probably due to the bulky *tert*-butyl groups. More interestingly, **3d** and **4d** have a higher ECL efficiency than their analogues (Table 2), and their ECL spectra can be fitted to two peaks (see the Supporting Information). The two peak wavelengths for **3d** and **4d** are listed in Table 2. While the first peak wavelength in ECL is very close to that in PL, the second peak can be assigned to emission from the excimer. Excimers are in fact the excited states of the dimer, which were observed in ECL of other organic compounds.[25,26] Excimers of **3d** and **4d** might be formed by dimerization of the radical anion and cation or stacking of a monomer in excited state with a monomer in ground state due to the long hexyl chains and π conjugation.

Note that the minimum energy needed to promote the silole to the excited state (Table 2, for instance, 435 nm, 2.86 eV from UV/Vis absorption peak wavelength of **4c**) is very close to the energy gap between the first oxidation and first reduction potentials (electrochemical energy gap) determined from the CV (Table 1, 2.47 eV for **4c**).

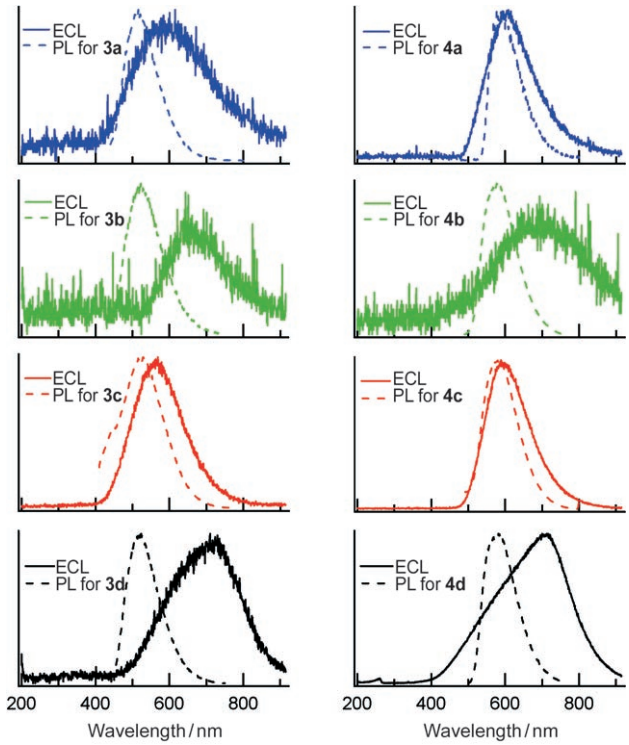

Figure 5. ECL (solid lines) and PL (dashed lines) spectra of the eight siloles. ECL and PL intensities were normalized by their respective peak heights.

In summary, structural modifications of thiophene–silole hybrid materials coupled with experimental tuning of electrochemical potentials and temporal pace gave rise to silole chromophores displaying efficient and stable ECL. By extending silole π conjugation with thiophene units and by constraining the applied potential range, stable radical cations favorable for ECL emission were generated. Further studies focusing on additional structural tuning, as well as other approaches to avoid electrode fouling, are underway.

Received: April 30, 2008
Revised: July 4, 2008
Published online: September 2, 2008

Keywords: chemiluminescence · electrochemistry · heterocycles · silicon · siloles

[1] S. Yamaguchi, K. Tamao, *J. Chem. Soc. Dalton Trans.* **1998**, 3693–3702.
[2] B.-H. Kim, H.-G. Woo, *Organometallics* **2002**, *21*, 2796–2798.
[3] M. Uchida, T. Izumizawa, T. Nakano, S. Yamaguchi, K. Tamao, K. Furukawa, *Chem. Mater.* **2001**, *13*, 2680–2683.
[4] S. Yamaguchi, T. Goto, K. Tamao, *Angew. Chem.* **2000**, *112*, 1761–1763; *Angew. Chem. Int. Ed.* **2000**, *39*, 1695–1697.
[5] S. Yamaguchi, T. Endo, M. Uchida, T. Izumizawa, K. Furukawa, K. Tamao, *Chem. Eur. J.* **2000**, *6*, 1683–1692.
[6] S. Yamaguchi, T. Endo, M. Uchida, T. Izumizawa, K. Furukawa, K. Tamao, *Chem. Lett.* **2001**, 98–99.
[7] J. Chen, C. C. W. Law, J. W. Y. Lam, Y. Dong, S. M. F. Lo, I. D. Williams, D. Zhu, B. Z. Tang, *Chem. Mater.* **2003**, *15*, 1535–1546.

[8] C. Liu, W. Yang, Y. Mo, Y. Cao, J. Chen, B. Z. Tang, *Synth. Met.* **2003**, *135–136*, 187 – 188.
[9] M. S. Liu, J. Luo, A. K.-Y. Jen, *Chem. Mater.* **2003**, *15*, 3496 – 3500.
[10] F. Wang, J. Luo, K. Yang, J. Chen, F. Huang, Y. Cao, *Macromolecules* **2005**, *38*, 2253 – 2260.
[11] G. Yu, S. Yin, Y. Liu, J. Chen, X. Xu, X. Sun, D. Ma, X. Zhan, Q. Peng, Z. Shuai, B. Tang, D. Zhu, W. Fang, Y. Luo, *J. Am. Chem. Soc.* **2005**, *127*, 6335 – 6346.
[12] B. Z. Tang, X. Zhan, G. Yu, P. P. S. Lee, Y. Liu, D. Zhu, *J. Mater. Chem.* **2001**, *11*, 2974 – 2978.
[13] X. Zhan, C. Risko, F. Amy, C. Chan, W. Zhao, S. Barlow, A. Kahn, J.-L. Bredas, S. R. Marder, *J. Am. Chem. Soc.* **2005**, *127*, 9021 – 9029.
[14] A. J. Boydston, Y. Yin, B. L. Pagenkopf, *J. Am. Chem. Soc.* **2004**, *126*, 3724 – 3725.
[15] A. J. Boydston, Y. Yin, B. L. Pagenkopf, *J. Am. Chem. Soc.* **2004**, *126*, 10350 – 10354.
[16] Electrogenerated chemiluminescence (ECL) is also called electrochemiluminescence: A. J. Bard, L. R. Faulkner, *Electrochemical Methods*, *Fundamentals and Applications*, 2nd ed., Wiley, New York, **2001**.
[17] M. M. Sartin, A. J. Boydston, B. L. Pagenkopf, A. J. Bard, *J. Am. Chem. Soc.* **2006**, *128*, 10163 – 10170.
[18] A. J. Boydston, B. L. Pagenkopf, *Angew. Chem.* **2004**, *116*, 6496 – 6498; *Angew. Chem. Int. Ed.* **2004**, *43*, 6336 – 6338.
[19] Reported absolute ECL efficiencies of DPA: a) 6.1% in acetonitrile, K. M. Maness, J. E. Bartelt, R. M. Wightman, *J. Phys. Chem.* **1994**, *98*, 3993 – 3998; b) 6.2–7.8% in mixturess of acetonitrile, benzene, and toluene: C. P. Keszthelyi, N. E. Tokel-Takvoryan, A. J. Bard, *Anal. Chem.* **1975**, *47*, 249 – 256.
[20] For reviews of ECL, see a) L. R. Faulkner, A. J. Bard in *Electroanalysis Chemistry*, *Vol. 10* (Ed.: A. J. Bard), Marcel Dekker, New York, **1977**, pp. 1 – 95; b) M. M. Richter, *Chem. Rev.* **2004**, *104*, 3003 – 3036; c) *Electrogenerated Chemiluminescence* (Ed.: A. J. Bard), Marcel Dekker, New York, **2004**.
[21] K. Tamao, M. Uchida, T. Izumizawa, K. Furukawa, S. Yamaguchi, *J. Am. Chem. Soc.* **1996**, *118*, 11974 – 11975.
[22] M. Katkevics, S. Yamaguchi, A. Toshimitsu, K. Tamao, *Organometallics* **1998**, *17*, 5796 – 5800.
[23] E. G. Janzen, J. B. Pickett, W. H. Atwell, *J. Organomet. Chem.* **1967**, *10*, P6 – P8.
[24] Y. Bae, N. Myung, A. J. Bard, *Nano Lett.* **2004**, *4*, 1153 – 1161.
[25] J.-P. Choi, K.-T. Wong, Y.-M. Chen, J.-K. Yu, P.-T. Chou, A. J. Bard, *J. Phys. Chem. B* **2003**, *107*, 14407 – 14413.
[26] R. Y. Lai, J. J. Fleming, B. L. Merner, R. J. Vermeij, G. J. Bodwell, A. J. Bard, *J. Phys. Chem. A* **2004**, *108*, 376 – 383.

